

Low-Cost CuInSe_2 Submodule Development

Final Subcontract Report
9 July 1990 – 31 January 1992

NREL/TP--413-5010

DE92 016438

B. M. Basol, V. K. Kapur, A. Halani,
C. Leidholm
International Solar Electric Technology
Inglewood, California

NREL technical monitor: H. S. Ullal



National Renewable Energy Laboratory
1617 Cole Boulevard
Golden, Colorado 80401-3393
A Division of Midwest Research Institute
Operated for the U.S. Department of Energy
under Contract No. DE-AC02-83CH10093

Prepared under Subcontract No. ZN-0-19019-2

October 1992

MASTER
ep

NOTICE

This report was prepared as an account of work sponsored by an agency of the United States government. Neither the United States government nor any agency thereof, nor any of their employees, makes any warranty, express or implied, or assumes any legal liability or responsibility for the accuracy, completeness, or usefulness of any information, apparatus, product, or process disclosed, or represents that its use would not infringe privately owned rights. Reference herein to any specific commercial product, process, or service by trade name, trademark, manufacturer, or otherwise does not necessarily constitute or imply its endorsement, recommendation, or favoring by the United States government or any agency thereof. The views and opinions of authors expressed herein do not necessarily state or reflect those of the United States government or any agency thereof.

Printed in the United States of America
Available from:
National Technical Information Service
U.S. Department of Commerce
5285 Port Royal Road
Springfield, VA 22161

Price: Microfiche A01
Printed Copy A03

Codes are used for pricing all publications. The code is determined by the number of pages in the publication. Information pertaining to the pricing codes can be found in the current issue of the following publications which are generally available in most libraries: *Energy Research Abstracts (ERA)*; *Government Reports Announcements and Index (GRA and I)*; *Scientific and Technical Abstract Reports (STAR)*; and publication NTIS-PR-360 available from NTIS at the above address.

DISCLAIMER

Portions of this document may be illegible electronic image products. Images are produced from the best available original document.

Abstract

This is the Final Report for a seventeen month research and development program entitled "Low Cost CuInSe₂ Submodule Development". The aim of this project is the development and demonstration of the processing steps necessary for the fabrication of high efficiency CuInSe₂ solar cells and sub-modules by the two-stage technique (also called the selenization method). During this period we have optimized the processing parameters of this method and demonstrated CuInSe₂/CdS/ZnO devices with 1-4 cm² area and up to 12.4 % active area efficiency. We have also developed a novel approach for the preparation of Cu/In precursors that improved the stoichiometric and morphological uniformity in these films. We have developed processing steps and tooling for handling up to 1 ft² size substrates and as a result of these efforts demonstrated our first monolithically integrated sub-module of 1 ft² area.

TABLE OF CONTENTS

	Page
Abstract	iii
List of Figures	v
List of Tables	vii
1.0 Summary	1
2.0 Introduction	2
3.0 Technical Discussion	2
3.1 Film Deposition and Analysis	2
3.1.1 Precursors	2
3.1.2 Selenization	9
3.2 Device Fabrication and Analysis	11
3.2.1 Window layers	13
3.2.2 Influence of the CdS deposition process on device charac- teristics	17
3.2.3 High efficiency cells	20
3.3 Fabrication of 1 ft ² Sub-Modules	22
3.3.1 Precursor preparation	22
3.3.2 Selenization	24
3.3.3 Window layer deposition	24
3.3.4 Module integration	25
3.3.5 Further work required on module processing	25
4.0 Conclusions	28
5.0 Acknowledgements	29
6.0 Future Plans	29
7.0 List of Publications	29
8.0 References	30

LIST OF FIGURES

- Fig. 1a. Surface SEM of a 500 Å thick In film evaporated over a Mo/glass substrate.
- Fig. 1b. Surface SEM of a 1500 Å thick In film on Mo/glass substrate.
- Fig. 2a. Cross sectional SEM of a precursor prepared by first evaporating an In film over a Mo/glass substrate and following this step by the evaporation of a Cu layer. Voids at the interface indicates poor adhesion.
- Fig. 2b. Cross sectional SEM of a precursor prepared by evaporating an In film on a Te/Mo/glass substrate and following this step by the evaporation of a Cu layer. The 20 Å thick Te layer affected both the morphology and the adhesion of the film.
- Fig. 3a. Surface SEM of a 500 Å thick In film evaporated over a Te/Mo/glass substrate. Te thickness was 20 Å.
- Fig. 3b. Surface SEM of a 1500 Å thick In film on Te/Mo/glass substrate. Te thickness was 20 Å.
- Fig. 4a. Precursor films prepared by ISET process have a completely intermixed Cu-In layer as seen in this Auger depth profile.
- Fig. 4b. In a In/Te/Mo/glass structure, Te distribution depends on the In evaporation rate. At high evaporation rates Te peak is at the Mo interface (1). If In deposition rate is low Te gets distributed more evenly through the growing film (2).
- Fig. 5a. SEM of a selenized film obtained from a glass/Mo/In/Cu precursor. Large grain areas were found to be Cu rich.
- Fig. 5b. SEM of a selenized film obtained from a glass/Mo/Te/In/Cu precursor. Stoichiometric and morphological uniformity of this film are good.
- Fig. 6. Reflectance, transmittance and absorption data obtained from CdS/glass samples.
- Fig. 7a. SEM of the surface of a chemically grown CdS layer showing crystallite over-growths.
- Fig. 7b. A close-up view of one of the crystallites of Fig. 7a.

- Fig. 8. Surface texture of a 2.5 μm thick ZnO film obtained by MOCVD.
- Fig. 9. Comparison of current losses for cells employing evaporated or chemically grown CdS windows.
- Fig. 10. Illuminated I-V characteristics of a 11.5% cell. The active area efficiency is 12.4%.
- Fig. 11. Quantum efficiency of the cell of Fig. 10.
- Fig. 12. Logarithmic plot of $J+J_L$ (\square) and dark I-V (\blacksquare) characteristics of the device of Fig. 10. Solid lines represent data corrected for R_s (0.2 and 0.3 $\Omega\text{-cm}^2$ in light and dark, respectively).
- Fig. 13. The sputtering system built for 1 ft^2 module processing.
- Fig. 14. Monolithic integration procedure for the modules.
- Fig. 15. Picture of a 1 ft^2 module processed in this program.
- Fig. 16. EBIC and SEI data taken from a $\text{CuInSe}_2/\text{CdS}/\text{ZnO}$ device. Some of the "low-response" areas on the EBIC photo can be correlated with physical features in the SEI.

LIST OF TABLES

Table 1. Parameters of cells with evaporated or dip coated CdS window layers. A is the diode quality factor of the device under illumination. Hole density, p, has been obtained by capacitance measurements.

1.0 SUMMARY

This is the Final Report for a seventeen month research and development program entitled "Low Cost CuInSe₂ Sub-module Development". The aim of this project is the development and demonstration of the processing steps necessary for the fabrication of high efficiency CuInSe₂ solar cells and sub-modules by the two-stage technique. The two-stage technique (also called the selenization method) involves; i) deposition of a Cu/In precursor film of controlled stoichiometry and morphology on a Mo-coated glass substrate, and ii) selenization of this precursor film to obtain a good quality CuInSe₂ layer. We had already demonstrated the feasibility of this process for the fabrication of high efficiency solar cells in our previous projects. Specifically, we had demonstrated small area (0.1 cm²) cells with active area efficiencies in the range of 10-11 % [1]. During this period we have further optimized the two-stage process and demonstrated devices with 1-4 cm² area and up to 12.4 % active area efficiency. We have also developed a novel approach for the preparation of Cu/In precursors that improved the stoichiometric and morphological uniformity in these films. We have studied the correlation between the nature of the precursors and the properties of the CuInSe₂ layers obtained after the selenization step. We have developed processing steps and tooling for handling up to 1 ft² size substrates and as a result of these efforts demonstrated our first monolithically integrated sub-module of 1 ft² area.

2.0 INTRODUCTION

The overall objective of this project is the development and demonstration of high efficiency CuInSe_2 solar cells and sub-modules by the two-stage technique. The specific goals are demonstration of 11% efficiency for 4 cm^2 devices and 8% efficiency for 1 ft^2 aperture area modules.

The two-stage technique (also called the selenization method) involves two separate processing steps. These are ; i) deposition of a Cu/In precursor film of controlled stoichiometry and morphology on a Mo-coated glass substrate, and ii) selenization of this precursor film to obtain a good quality CuInSe_2 layer. The elemental layers in a two-stage process can be deposited by various techniques. In this project we have used the E-beam evaporation method for the small area device processing and magnetron sputtering for the 1 ft^2 module work. Selenization in both cases was carried out in an H_2Se atmosphere at around $400 \text{ }^\circ\text{C}$. The following sections of this report will discuss the film and cell processing steps as well as the characteristics of the resulting films and devices.

3.0 TECHNICAL DISCUSSION

3.1 Film Deposition and Analysis

Two-stage process was used for the deposition of the CuInSe_2 films on Mo coated glass substrates. The Mo layers used in this work were deposited on soda-lime glass sheets by the sputtering technique. High efficiency device work was carried out using CuInSe_2 films obtained by the E-beam evaporation/selenization approach. Modules were fabricated by the sputtering/selenization technique. In this section we will concentrate on the E-beam evaporated films. Sputtering approach and the processing of large area modules will be presented in Section 3.3.

3.1.1 Precursors

The quality of the CuInSe_2 layers obtained by the two-stage process depends on the kinetics of the selenization process as well as the nature of the Cu-In precursor films. The degree of alloying between the Cu and In films, their morphology and compositional uniformity are some of the important factors that determine the nature of a CuInSe_2 layer obtained by using the selenization technique. Morphological and stoichiometric non-uniformities present in the precursor films generally manifest themselves as electrically active defects in the reacted compound layers. For the case of depositing binary compounds like CdTe using the two-stage process,

localized stoichiometric non-uniformities in the elemental Cd/Te stacks give rise to pinholes or thickness variations in the CdTe films after the reaction step. These defects result from the evaporation of localized excess Te or Cd out of the compound layer at the elevated temperatures (>400 °C) that are commonly employed for processing these materials. For the case of CuInSe_2 , the situation is further complicated by the existence of non-volatile phases such as Cu_xSe , In_2Se_3 , $\text{Cu}_2\text{In}_4\text{Se}_7$ and CuIn_3Se_5 , which may result from the compositional non-uniformities present in the un-selenized Cu-In films. Among these compounds the Cu_xSe phase is the most detrimental to solar cell performance because of its low resistivity. If present in the CuInSe_2 layer, this phase causes excessive leakage in devices fabricated on such a layer. It is essential that the Cu-In precursors used for selenization be free of gross stoichiometric and morphological non-uniformities and that they adhere well to their substrates. In this research program we have developed a new approach to the preparation of high quality precursor layers and demonstrated their use in the selenization technique to obtain compositionally and morphologically uniform CuInSe_2 films.

In these experiments we used the E-beam evaporation method for the deposition of the metallic precursors (1,2,3). Cu and In films were sequentially evaporated onto Mo coated soda-lime glass substrates at pressures of around 2×10^{-5} Torr. Sequence of deposition was varied to study possible structural effects in the resulting films. In some experiments, a thin layer of Te was electrodeposited on the Mo surface before the evaporation of the precursor films to demonstrate the influence of such a Mo surface modification approach on the quality of the resulting Cu-In layers. A coulombmeter was used to control the thickness of the electrodeposited Te layer in these experiments. Cu and In film thicknesses were controlled with the help of a quartz oscillator.

a) Commonly used Cu/In precursors:

The commonly used process for the preparation of a Cu-In precursor for selenization involves depositing a thin Cu layer on a glass/Mo substrate and then following this step with the deposition of an In film (4,5,6). For a Cu-to-In ratio of 0.95, the typical thicknesses of the Cu and In layers are 1500-2000 Å and 3500-4600 Å, respectively.

There are two reasons for the preference of the Cu/In precursor structure over the In/Cu deposition sequence. The first reason is process related and it is especially valid for the case of electrodeposited Cu/In stacks. If the Cu and In films are electrodeposited out of the commonly used Cu-sulfate and In-sulfamate electrolytes (7), then the chemical potential considerations require that the Cu layer be plated first onto the Mo coated substrate. If the reverse is attempted, then the stoichiometric

control is lost because In, which has a standard reduction potential of -0.33 V partially dissolves into the plating electrolyte during the Cu deposition step. It should be noted that the standard reduction potential of Cu is $+0.34$ V.

The second reason for the wide usage of the glass/Mo/Cu/In structure for selenization is related to the morphological and mechanical properties of the precursor films. Cu layers evaporated onto Mo coated glass substrates at room temperature have a small grained structure and they form smooth and continuous layers with adequate adhesion to the Mo surface. After the indium deposition step these precursors are partially alloyed (1,2,6) and they still adhere reasonably well to their Mo coated glass substrates. The properties of these Cu/In layers strongly depend on the deposition parameters of their elemental components. In the case of evaporation, low In deposition rates and fine-grain copper layers enhance the degree of alloying between the Cu and In films (6). Substrate heating also affects the microstructure of the individual elemental layers as well as the morphology and the alloy phase composition of the resulting precursor. Intermixing between Cu and In also takes place during the selenization step which involves high temperature annealing. As can be seen from this brief discussion the properties of evaporated Cu/In precursor layers can be quite varied depending upon their many preparation conditions. This can cause poor repeatability for the CuInSe_2 film characteristics which are affected by the nature of the precursor layers. The purpose of our work was to develop a new approach to Cu-In film preparation, where an extensively alloyed precursor layer could be obtained within a reasonably wide range of deposition parameters. The following section will discuss this novel approach which yielded high quality precursor films and CuInSe_2 layers.

b) In/Cu precursors developed by ISET:

In our previous reports we pointed out that the degree of alloying between the evaporated Cu and In films depend, among other factors, on the sequence of deposition (1). Specifically, we indicated that evaporating Cu over an In layer which has a low melting point, gave rise to more complete intermixing between the two elements. Recognizing that a completely alloyed precursor which could be prepared in a repeatable manner would offer advantages over those whose properties change from batch to batch, we initiated work on developing In/Cu precursors where the In layer was deposited first on the Mo surface.

The SEMs of Fig. 1a and Fig. 1b show the evolution of the microstructure of an In film evaporated on a Mo coated glass substrate. The micrograph in Fig. 1a was taken from a 500 \AA thick In film deposited on the Mo surface and it clearly demonstrates the poor nucleation characteristics of In on that material. At this

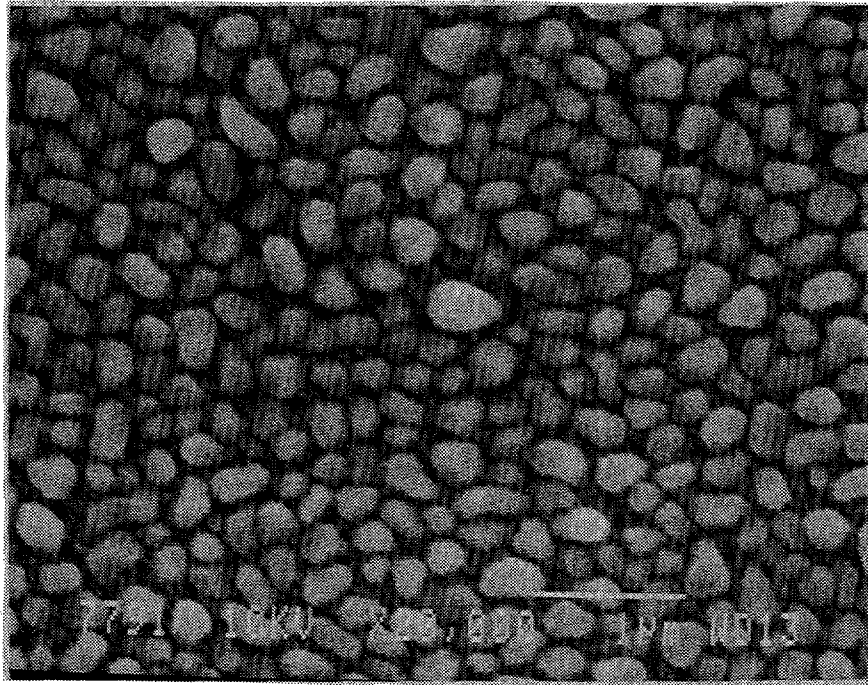


Fig. 1a. Surface SEM of a 500 Å thick In film evaporated over a Mo/glass substrate.

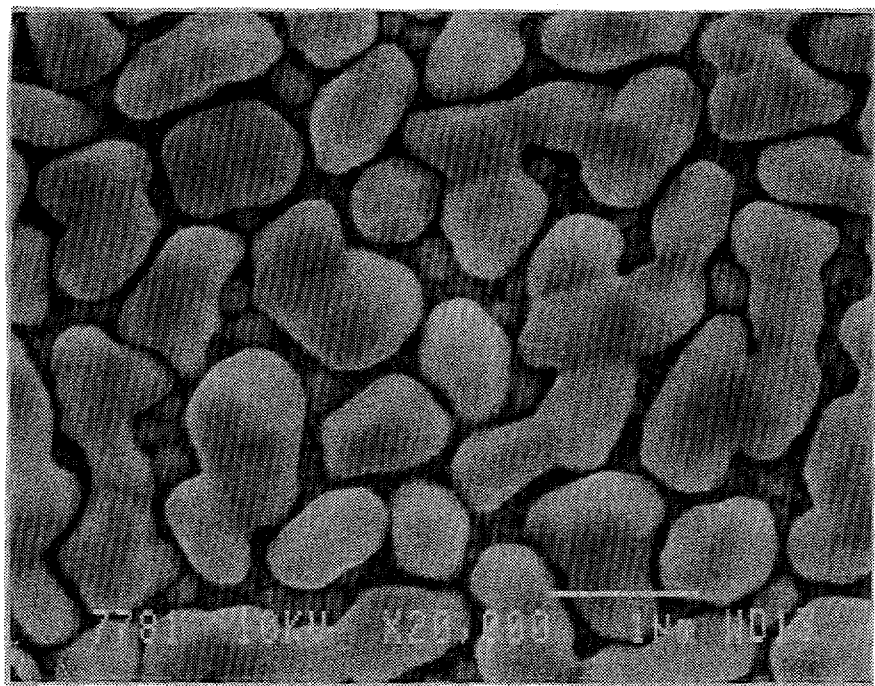


Fig. 1b. Surface SEM of a 1500 Å thick In film on Mo/glass substrate.

thickness, the In film was in the form of isolated droplets of 0.1-0.5 μm size. These droplets grew larger in a film with a thickness of 1500 \AA (Fig. 1b) and for thicknesses >2000 \AA they melted together to form a continuous film. The resulting layer was reflective and it displayed a relatively smooth surface topography (8). Although the surface structure of this film appeared to be uniform, its bond with the underlying Mo layer was poor. Failure of this weak bond often caused film peeling after the Cu evaporation step as observed by us and also reported by others (5).

Characteristics of thin films, among other factors, depend on the nature of the interfacial region at the substrate/film interface (9). The nature of this region, on the other hand, is determined by the chemical interactions between the depositing species and the substrate material. Mo is a relatively inert metal. In fact, this was the major reason for its selection as the ohmic contact to CuInSe_2 thin films which are generally grown in reactive environments. Lack of chemical interaction between Mo and In results in an "abrupt" interface and a weak bond between these two metals. After the evaporation of Cu, this bond often breaks and precursors partially peel off their substrates even before the selenization step. Fig. 2a is the SEM of such a glass/Mo/In/Cu structure. It is observed that evaporation of a Cu film over a 4000-5000 \AA thick In layer transformed this smooth looking layer into a precursor with a highly non-uniform microstructure and poor adhesion, which is indicated by the large voids seen at the Mo/film interface. When selenized, such precursors gave poorly adhering CuInSe_2 films that often displayed structural and morphological non-uniformities as will be shown in the next section.

Since the properties of thin films are influenced by the character of the substrate/film interface, it is possible to alter these properties by modifying the substrate surface. In our two-stage process, this can be achieved by interjecting a thin interfacial layer between the depositing In film and the Mo coated substrate. In doing so, however, it is important to assure that the elements included in this inter-facial layer do not adversely affect the electrical properties of the CuInSe_2 film obtained after the selenization step.

Te is a group VI material like Se. It can be deposited by a variety of methods such as evaporation, sputtering and electrodeposition. Diffusion of Te has been shown to enhance the p-type character of CuInSe_2 crystals (10). Furthermore, Te reacts with In forming various compounds (11). Therefore, a thin Te layer deposited on the Mo surface is expected to influence the nucleation characteristics of a subsequently evaporated In film. In our experiments we have successfully used 20-200 \AA thick Te interfacial films to improve the quality of the evaporated In/Cu precursors and to optimize the structural, mechanical and electrical properties of the CuInSe_2 layers obtained utilizing these precursors.

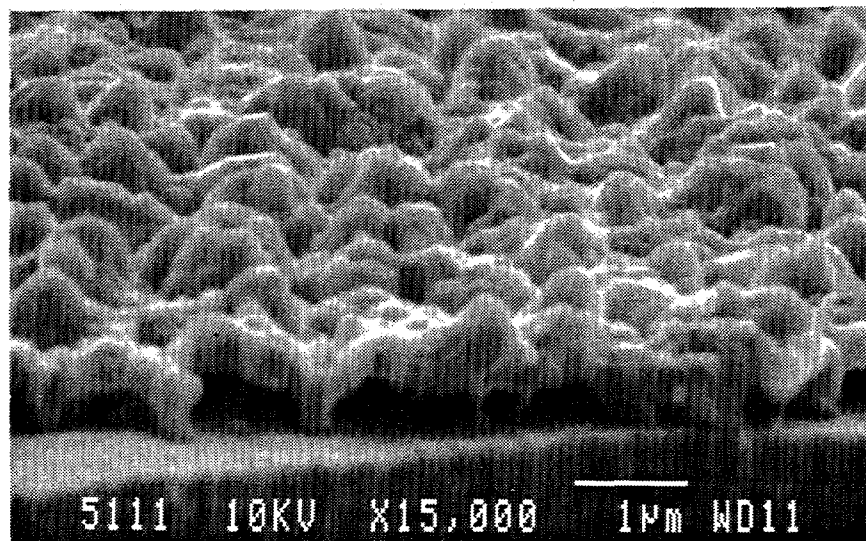


Fig. 2a. Cross sectional SEM of a precursor prepared by first evaporating an In film over a Mo/glass substrate and following this step by the evaporation of a Cu layer. Voids at the interface indicates poor adhesion.

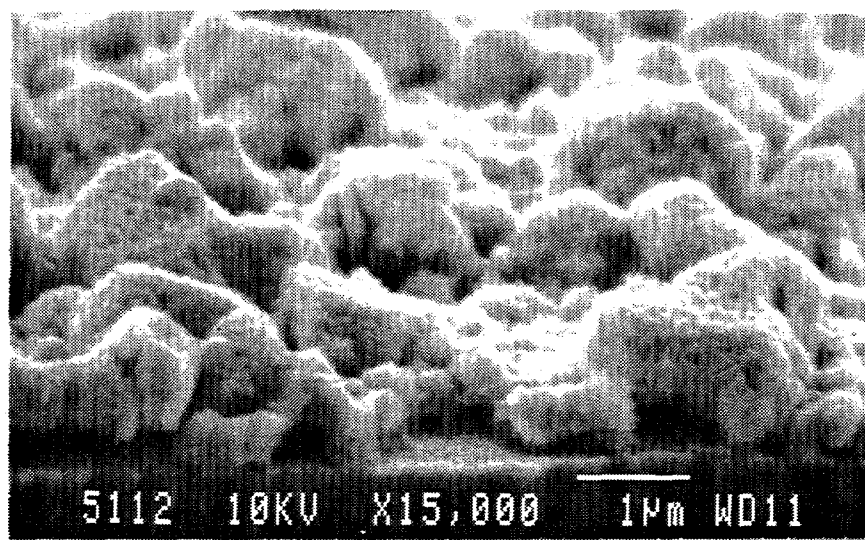


Fig. 2b. Cross sectional SEM of a precursor prepared by evaporating an In film on a Te/Mo/glass substrate and following this step by the evaporation of a Cu layer. The 20 Å thick Te layer affected both the morphology and the adhesion of the film.

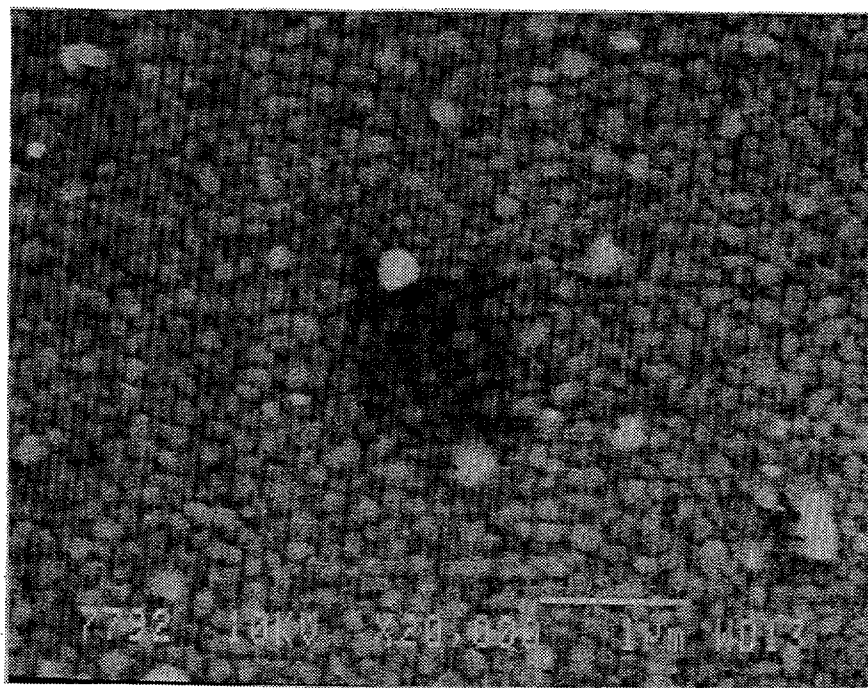


Fig. 3a. Surface SEM of a 500 Å thick In film evaporated over a Te/Mo/glass substrate. Te thickness was 20 Å.

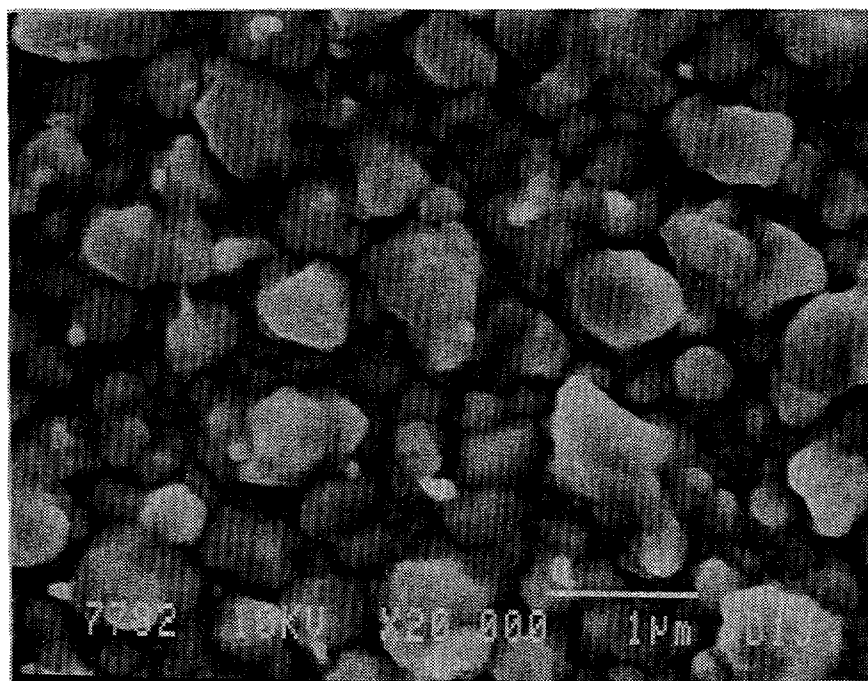


Fig. 3b. Surface SEM of a 1500 Å thick In film on Te/Mo/glass substrate. Te thickness was 20 Å.

The SEMs of Figs. 3a and 3b demonstrate the effect of a 20 Å thick electrodeposited Te interfacial layer on the morphology of In films evaporated on Mo coated glass substrates. When compared with the sample of Fig. 1a, the 500 Å thick In layer deposited on the Te/Mo/glass substrate (Fig 3a) was found to have much smaller grains, and it formed a continuous film even at this small thickness. This observation implies that the wetting and the coverage of the substrate surface by In were appreciably improved by the presence of a thin Te film. Fig. 3b shows the morphology of the same film as its thickness was increased to 1500 Å. When compared with the SEM of Fig. 1b, this data indicates a better coverage of In and various size grains rather than large droplets as it was the case in Fig. 1b. Unlike an In layer deposited directly on the Mo surface, the micro-structure of the In film deposited over the Te-modified Mo surface was non-specular even after its thickness reached over 2000 Å. When a Cu layer was deposited over this glass/Mo/Te/In structure, the film shown in Fig. 2b was obtained. A direct comparison of the SEM's in Figs. 2a and 2b demonstrates the differences between these two precursors. Introduction of a thin Te layer at the substrate/film interface has provided a precursor film with much smaller grain structure, better coverage and better adhesion to the substrate.

In the above examples we have demonstrated that a thin interfacial layer of Te deposited on the Mo surface has improved the mechanical and structural properties of the evaporated precursor films. The chemical modification of the Mo surface was also found to facilitate a near-complete alloying between the In and Cu layers as demonstrated in the Auger depth profile of Fig. 4a. This data was taken from a sample with Te, In and Cu thicknesses of 150 Å, 2400 Å and 1000 Å, respectively, and it shows uniform distributions of Cu and In through the precursor layer. It is also noted that the Te peak is localized near the Mo interface of this sample which was prepared using an In evaporation rate of 20 Å/sec. We found that lower In evaporation rates enhanced the diffusion of Te into the growing In film and resulted in a more distributed Te profile. This can be seen from the Auger data of Fig. 4b which compares the Te distributions in two In/Te/Mo/glass structures prepared using two different In evaporation rates.

3.1.2 Selenization

After the evaporation of In and Cu layers, substrates were placed in a reactor and the metallic layers were selenized in a H₂Se atmosphere for about 1 hour. The selenization temperature was kept at around 400 °C. As a result of this reaction step, samples of glass/Mo/CuInSe₂ were obtained. The characteristics of the precursor layers and the selenized films were correlated by SEM studies.

We had already pointed out that the morphology of a CuInSe₂ layer

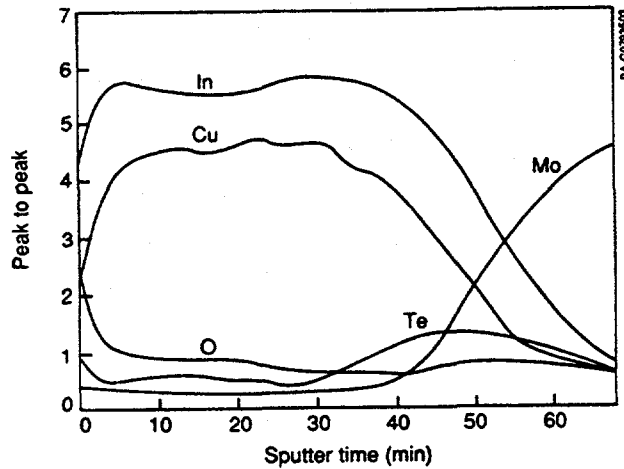
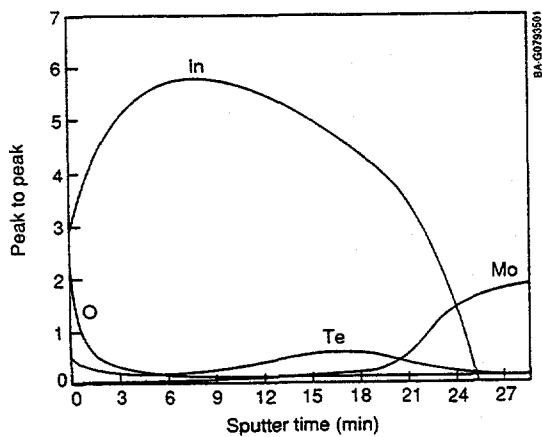
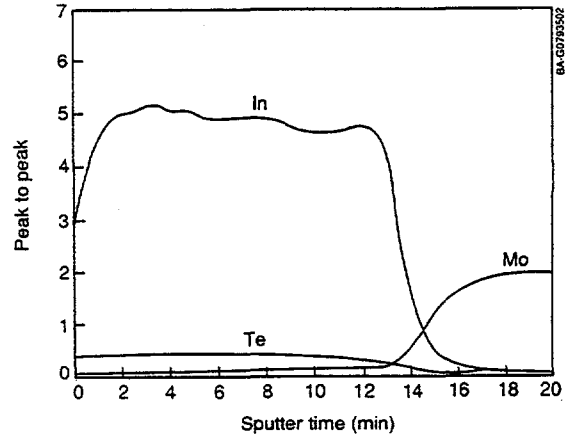


Fig. 4a. Precursor films prepared by ISET process have a completely intermixed Cu-In layer as seen in this Auger depth profile.



(1)



(2)

Fig. 4b. In a In/Te/Mo/glass structure, Te distribution depends on the In evaporation rate. At high evaporation rates Te peak is at the Mo interface (1). If In deposition rate is low Te gets distributed more evenly through the growing film (2).

grown by the two-stage technique is a strong function of the nature of the precursor film used for selenization. Specifically, we had shown that electrodeposited Cu/In precursors yielded films with large grains of $>1\mu\text{m}$ size, whereas, the grain size of CuInSe_2 layers obtained from alloyed Cu-In precursors could be sub-micron especially for highly In-rich compositions. We also suggested that the reason for this observation was the existence of a liquid In phase in the precursors prepared by the electrodeposition technique which promoted grain growth (2).

Besides their grain size, the stoichiometric and morphological uniformity of CuInSe_2 layers also depend on the nature of the precursor films. As we discussed in the previous section, the precursor layers can be prepared by various approaches, the most common one being deposition of an In layer over a Cu film. In the approach we developed In is first deposited on a Mo surface that has a thin layer of Te over it. This step is then followed by the evaporation of the Cu layer. The effect of the Te inter-layer on the quality of the resulting CuInSe_2 film can be understood from the SEM data of Figs. 5a and 5b. Fig. 5a was obtained from a CuInSe_2 layer obtained by the selenization of a glass/Mo/In/Cu structure and it shows large, Cu-rich grains imbedded into a small-grained background. Upon examination by microprobe these large grain areas were found to contain Cu_xSe phase. Solar cells fabricated on such layers had poor open circuit voltage values and low fill factors.

Selenization of glass/Mo/Te/In/Cu precursors on the other hand, resulted in CuInSe_2 films similar to that shown in Fig. 5b (12). The microstructure of this layer is uniform and its contrast to the SEM of Fig. 5a is very clear. When used in device fabrication, these uniform CuInSe_2 films yielded cells with good fill factors and open circuit voltages of > 0.45 V. We have used the processing approach described in this report to fabricate CuInSe_2 solar cells with over 12% active area efficiency.

3.2 Device Fabrication and Analysis

Solar cells were fabricated using CdS/ZnO window layers. The CdS films were either evaporated or chemically grown. Possible effects of CdS processing on the device behavior was studied. For evaporation high-purity, un-doped CdS crystals were used as the source material. The substrate temperature and the rate of evaporation were 200°C and $50\text{-}80 \text{ \AA}/\text{sec}$, respectively. The chemically grown CdS layers were obtained using the well established meta-stable electrolytes containing Cd salt, a sulfur source and a complexing agent. ZnO films were deposited using a MOCVD technique with diethyl zinc as the Zn source. The CdS and ZnO films were also deposited on witness glass substrates for optical and electrical evaluation. Optical measurements were made using an integrating sphere to obtain total reflectance and transmittance

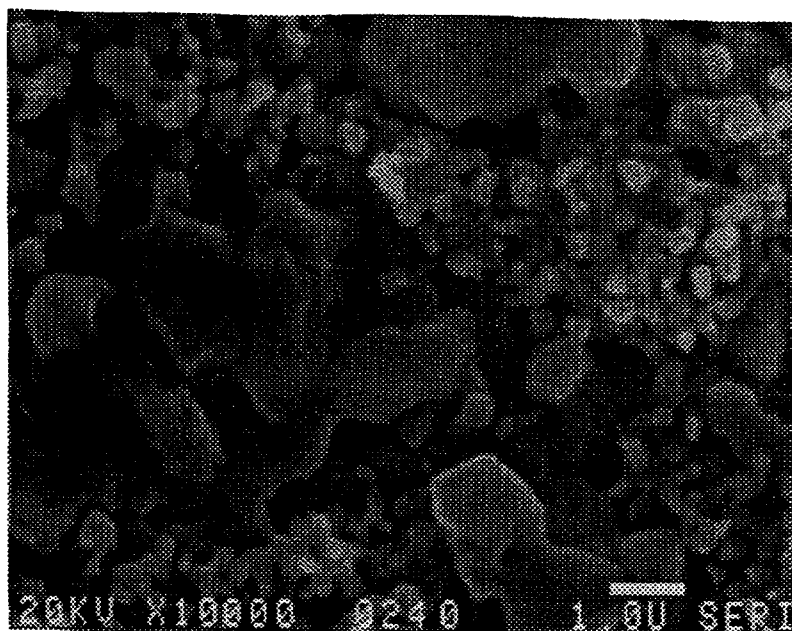


Fig. 5a. SEM of a selenized film obtained from a glass/Mo/In/Cu precursor. Large grain areas were found to be Cu rich.

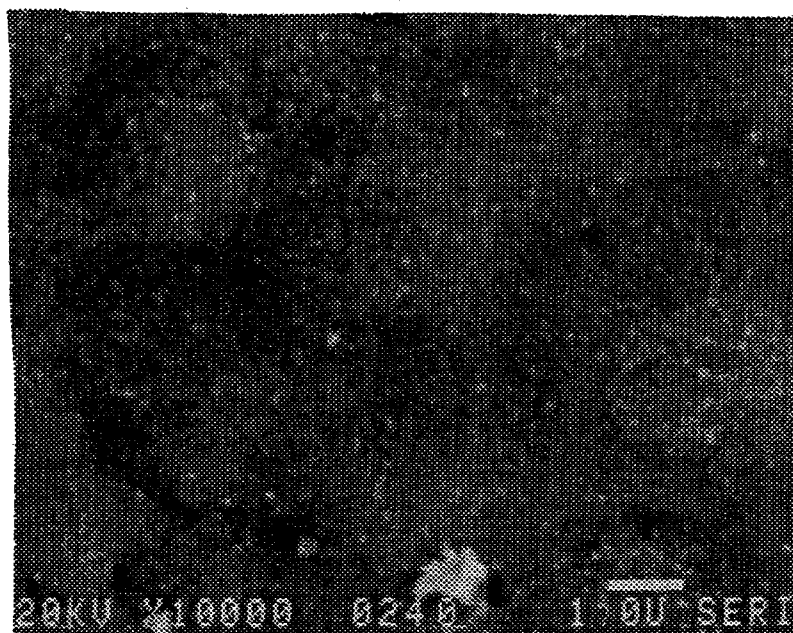


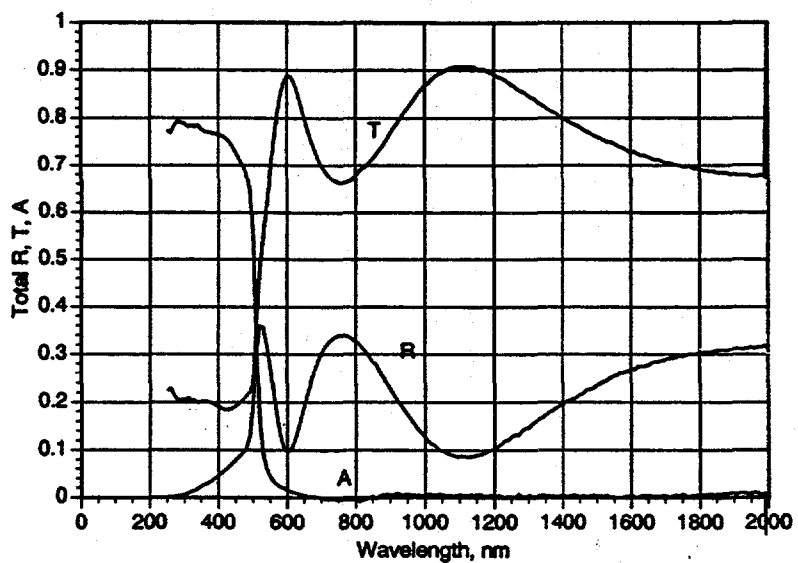
Fig. 5b. SEM of a selenized film obtained from a glass/Mo/Te/In/Cu precursor. Stoichiometric and morphological uniformity of this film are good.

values. Diffuse components of these parameters were also measured. Devices were characterized by spectral response, I-V and C-V measurements.

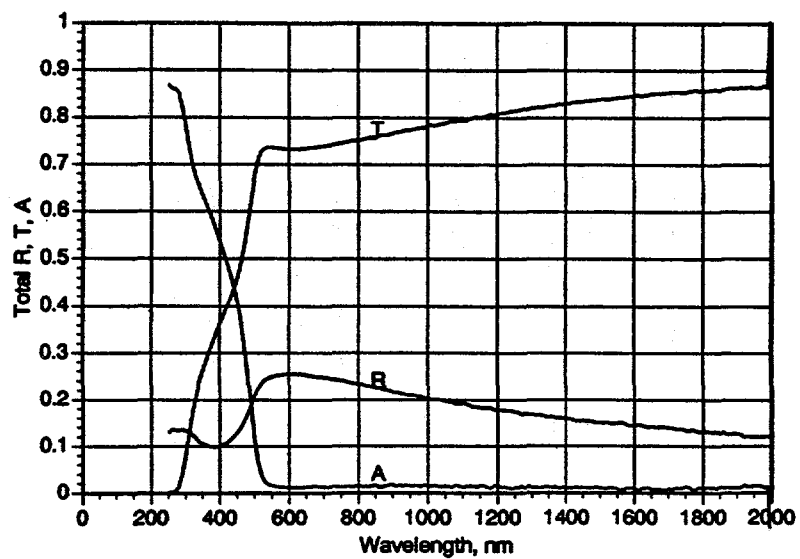
3.2.1 Window layers

Evaporated and chemically grown CdS layers deposited on glass substrates were evaluated in terms of their optical properties. Fig. 6 shows the transmittance, reflectance and absorption characteristics of a 0.24 μm thick evaporated CdS film (a) and a 0.2 μm thick chemically grown layer (b). It is observed that the optical transmission of the chemically grown CdS layer is relatively high even at energies greater than the absorption edge which is at around $\lambda=0.52 \mu\text{m}$. This is a result of the low reflectance and the low absorption displayed by these films. The reflectance of the chemically grown CdS film of Fig. 6, for example, is about half of what we measured for the evaporated layer in the same wavelength range of $0.3 \mu\text{m} < \lambda < 0.5 \mu\text{m}$. Similarly, the absorption of the chemically grown layer at 0.4 μm is only 54% compared to 76% for the evaporated film. Ellipsometry studies made on chemically deposited CdS showed a lower than expected index of refraction value (1.8-2.0 compared to 2.3 for evaporated layers) which explains the measured low reflectance. One other difference between the evaporated and chemically coated CdS films was their resistivity values. The in-plane resistivity of the dip coated layers was $>10^5 \Omega\text{-cm}$, whereas, this value was in the 100-500 $\Omega\text{-cm}$ range for the evaporated films. This is partly due to stoichiometric differences. The chemically deposited CdS layers are highly stoichiometric compared to the evaporated layers. The evaporated films, under the present deposition conditions, had a slight Cd-excess giving them a darker yellow color compared to the dip coated layers. The other factor influencing the conductivity of the dip-coated CdS films may be the presence of chemically adsorbed oxygen which is expected to decrease the measured in-plane conductivity of such films. All of these factors and possible structural variations contribute to the differences observed in the properties of the evaporated and chemically deposited CdS thin films.

The microstructure of a chemically grown CdS layer depends on the temperature and the chemical composition of the deposition electrolyte. High temperatures and bath compositions promoting a high rate of reaction between the cadmium and sulfur species, generally result in the formation of large CdS crystallites on the otherwise smooth and small-grained base film. The SEM of Fig. 7a shows some of these 10-20 μm size crystallites. If the density of these formations increase, the CdS layers become extremely rough, and the diffuse component of the optical transmission through such films increase. An in-depth study of the crystallites has shown that they were not just loosely attached to the surface of the grown film but they actually had grown out of the film. The SEM of



(a) 0.24 μm thick CdS film by evaporation.



(b) 0.2 μm thick CdS film by chemical deposition.

Fig. 6. Reflectance, transmittance and absorption data obtained from CdS/glass samples.

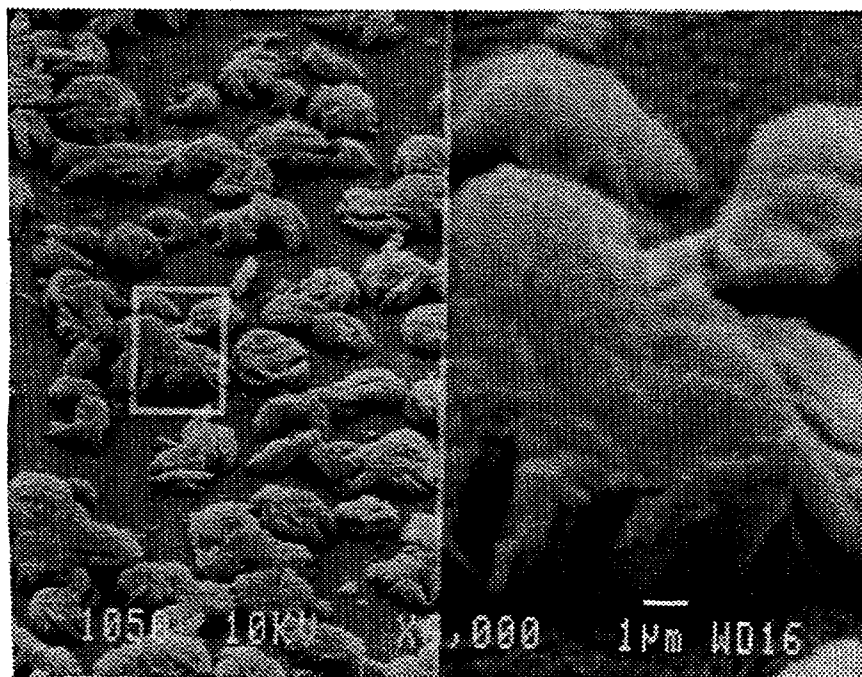


Fig. 7a. SEM of the surface of a chemically grown CdS layer showing crystallite over-growths.

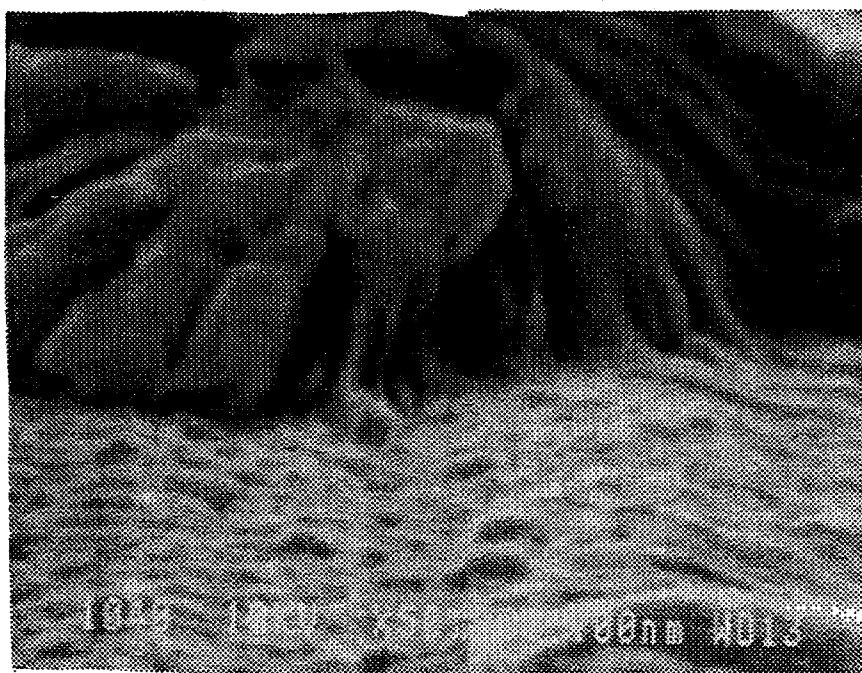


Fig. 7b. A close-up view of one of the crystallites of Fig. 7a.

Fig. 7b is a close-up view of one of the crystallites showing the interface between the smooth CdS film surface and the over-growth. The continuity in the structure around the edges of the over-growth suggests that its growth was initiated early in the film deposition period. Removal of this crystallite by mechanical means using a cotton swab left behind a hole that extended all the way down to the glass surface. The microstructure of the chemically grown CdS layers can be varied to eliminate excessive crystallite growth by controlling the deposition temperature, the concentrations of the cadmium and sulfur species and the amount of complexing agent introduced into the bath. Conditions promoting fast growth such as inadequate amount of complexing agent, high temperature and high thiourea content generally also promote crystallite over-growth. We were able to control these parameters to obtain highly uniform films with thicknesses ranging from 500 Å to 2500 Å.

The SEM of Fig. 8 shows the surface topography of a 2.5 μm thick ZnO film grown by the MOCVD technique. The surface is textured with 0.5-1.0 μm size features and the film is "milky" in appearance. Optical characteristics of these layers and their influence on the J_{sc} values of solar cells were carefully studied and the results have been published in reference (13). The surface texture of the ZnO layers can be varied by controlling the DEZ/oxidant ratio in the reactor. We have not yet determined a clear correlation between the device performance and the texture of the ZnO layer used in that device.

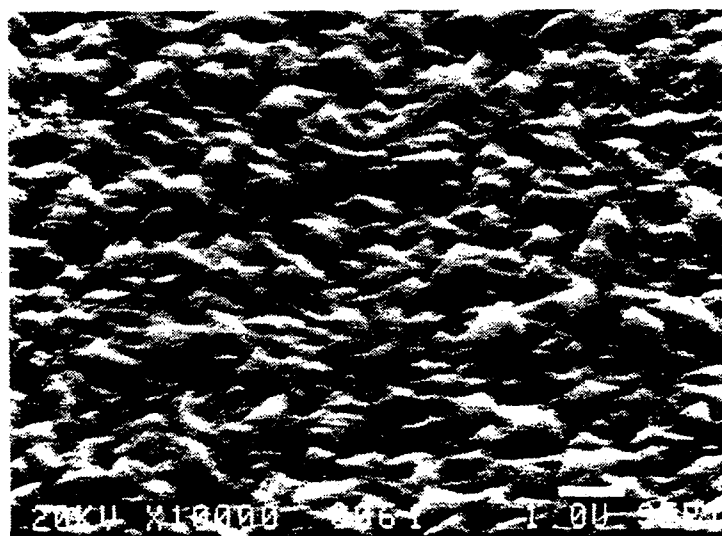


Fig. 8. Surface texture of a 2.5 μm thick ZnO film obtained by MOCVD.

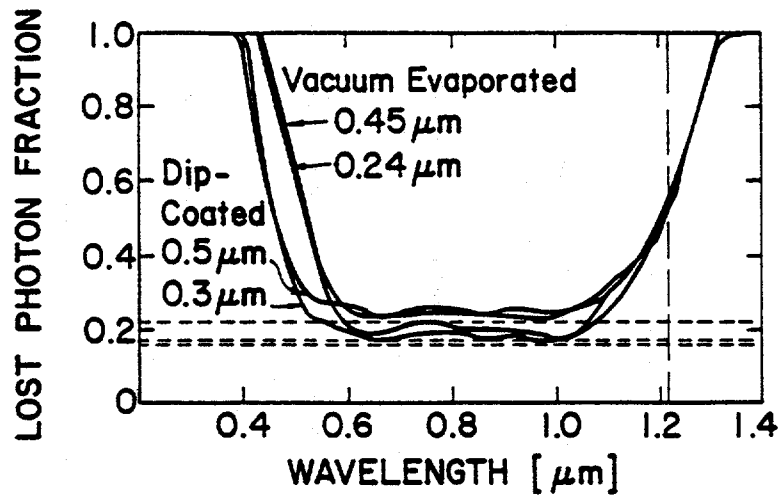
3.2.2. Influence of the CdS deposition process on device characteristics

In a previous publication, we had pointed out that good quality junctions could be formed on CuInSe_2 films of a wide range of stoichiometries using the chemically grown CdS layers (1). Experiments made on near-stoichiometric CuInSe_2 films had demonstrated that devices employing a chemically grown inter-layer of CdS placed between the CuInSe_2 film and the evaporated CdS window layer displayed higher V_{oc} values compared to those with just evaporated CdS layers. In this work, we studied the current loss mechanisms as well as the junction qualities of some ZnO/CdS/CuInSe_2 structures where the 0.2-0.5 μm thick CdS windows were obtained by either the evaporation technique or the chemical dip method.

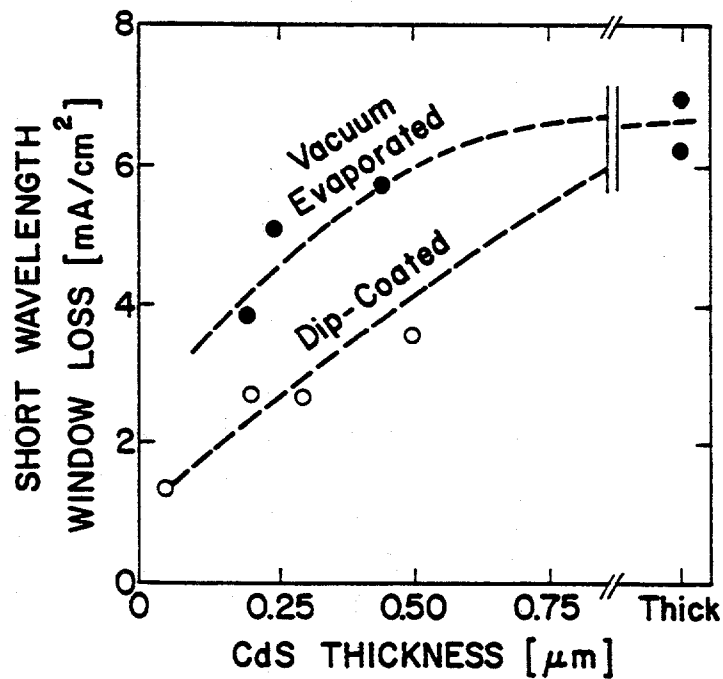
Fig. 9a shows the lost photon fraction of a set of devices prepared with evaporated and chemically grown CdS windows. The wavelength independent losses observed in the 0.6 μm $< \lambda <$ 1.0 μm range in these cells are due partly to reflection and partly to absorption in the ZnO layers. These losses do not show any clear relation to the method of CdS deposition. The short wavelength response, on the other hand, correlates well with the technique used to coat the CdS windows. Fig. 9b plots the short wavelength window losses for a group of ZnO/CdS/CuInSe_2 cells. It is observed that the devices with chemically grown CdS films generate about 2 mA/cm^2 more photocurrent than the evaporated CdS films even for CdS thicknesses of around 0.5 μm . This is consistent with the optical data we presented in the previous section which showed higher photon transmission in chemically deposited CdS layers. It is also possible that collection of photo-generated carriers from the highly resistive chemically deposited CdS layers contribute to the enhanced photo currents observed in these devices.

CdS film optical and electrical properties are not the only factors affecting the characteristics of the ZnO/CdS/CuInSe_2 solar cells studied in this work. The processes used in the deposition of the CdS and ZnO films are also expected to influence the quality of these junctions. For example, the chemical growth method allows the deposition of extremely thin ($< 0.05 \mu\text{m}$) CdS films on rough CuInSe_2 surfaces in a conformal manner. In the evaporation approach, discontinuities in thin CdS layers and their thickness control present practical problems. Furthermore, evaporation requires heating the CuInSe_2 films to around 200 $^\circ\text{C}$ in vacuum which may cause loss of Se from the surface layer. During the early phases of deposition the CuInSe_2 surface is also exposed to the incoming elemental Cd and S vapors which react to form the CdS compound. Chemical method is a low-temperature approach that allows the growth of a stoichiometric compound film on the CuInSe_2 surface at temperatures $< 80 \text{ }^\circ\text{C}$.

We have studied the possible influence of the CdS deposition



(a) Loss photon fraction for a group of cells.



(b) Window loss vs CdS thickness for evaporated and chemically deposited CdS layers.

Fig. 9. Comparison of current losses for cells employing evaporated or chemically grown CdS windows.

techniques on the junction quality of ZnO/CdS/CuInSe₂ structures. For this purpose, we have carried out controlled experiments in which the same CuInSe₂ film was used in the fabrication of solar cells employing either a chemically coated or an evaporated CdS window layer. We have consistently measured lower diode factors, better fill factors (after taking out the series resistance effect) and higher open-circuit-voltages for the dip coated samples. Capacitance measurements showed that the dip coated CuInSe₂ films displayed higher hole density values than those coated with evaporated CdS windows. This observation points to a significantly reduced compensation in the junction areas of cells using the dip coated CdS layers. A list of the relevant parameters for a group of devices and their structures are given in Table 1. The observed correlation between the CdS deposition technique and these parameters is very good. The increased degree of compensation in the films with evaporated window layers may be due to their exposure to the elemental Cd vapor at relatively high temperatures in the vacuum chamber.

Cell #	Window	A	FF	p(cm ⁻³)	Eff.(%)
629-1	0.20 μm evap.	1.95	0.56	1.3x10 ¹⁶	5.6
629-2	0.20 μm dip	1.60	0.70	3.0x10 ¹⁶	10.4
673-1	0.24 μm evap.	1.90	0.56	1.0x10 ¹⁶	7.4
673-2	0.45 μm evap.	1.75	0.63	1.2x10 ¹⁶	8.6
673-3	0.50 μm dip	1.70	0.68	3.0x10 ¹⁶	10.4

Table 1. Parameters of cells with evaporated or dip coated CdS window layers. A is the diode quality factor of the device under illumination. Hole density, p, has been obtained by capacitance measurements.

3.2.3. High Efficiency Cells

Fig. 10 is the illuminated I-V characteristics of a 1 cm² area device with 11.5 % total area efficiency measured at SERI under AM1.5 global spectra. The solar cell parameters of this device are; $V_{oc} = 0.4832$ V, $J_{sc} = 35.60$ mA/cm² and FF=66.65 %. The active area efficiency is 12.4 % as calculated by us. The quantum efficiency curve of Fig. 11 shows the 360 nm cutoff which is due to the ZnO bandgap, a shoulder at around 500 nm that is due to the thin CdS layer and a long wavelength cutoff extending to over 1.2 μ m. The peak of the quantum efficiency is 85%. The J_{sc} value of this cell was limited by the reflection losses (about 5%), absorption in the ZnO and CdS layers (around 10%) and both ZnO absorption and carrier collection losses at longer wavelengths. The $\ln(J+J_{sc})$ data superimposed over the dark I-V characteristics of the cell is shown in Fig. 12. Data after the series resistance correction for both curves is also included in this figure. It is observed that the voltage shift commonly observed between the light and dark I-V characteristics of CuInSe₂ solar cells is small (<15 mV) in this device indicating good junction quality. The diode quality factors in the dark and under illumination are 1.6 and 1.8 respectively. The capacitance measurements made on this device yielded a carrier density of around 2×10^{16} cm⁻³ and very small frequency dispersion, again indicating good junction quality. The best diode quality factor and the highest hole density measured for our devices were 1.50 and 7×10^{16} cm⁻³, respectively (14).

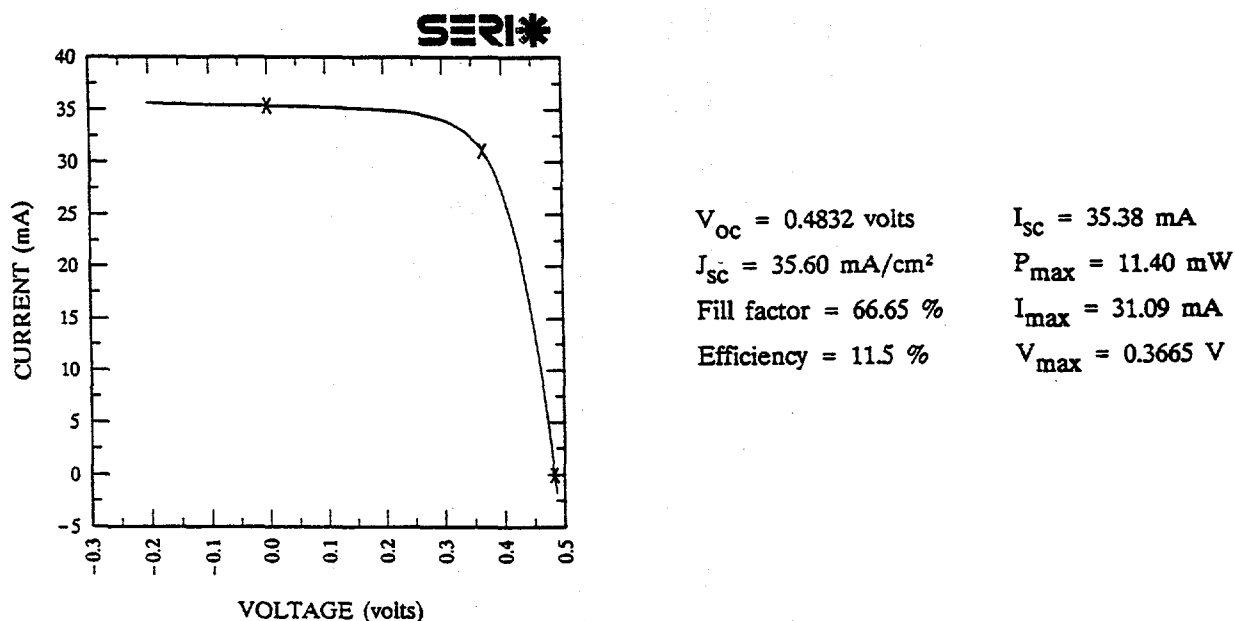


Fig. 10. Illuminated I-V characteristics of a 11.5% cell. The active area efficiency is 12.4%.

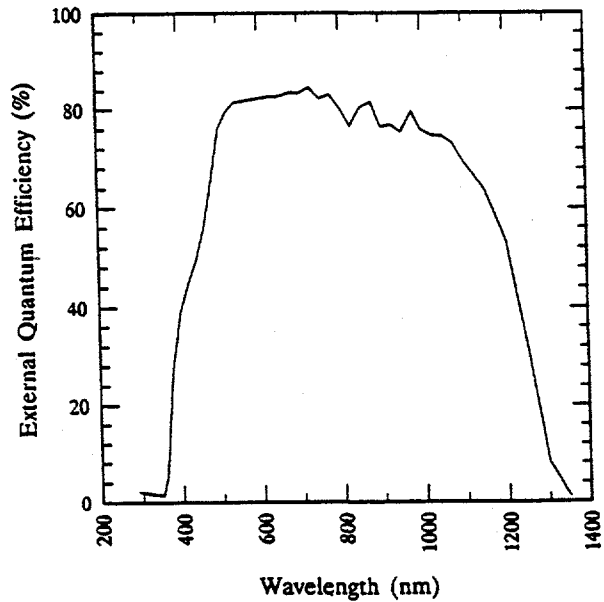


Fig. 11. Quantum efficiency of the cell of Fig. 10.

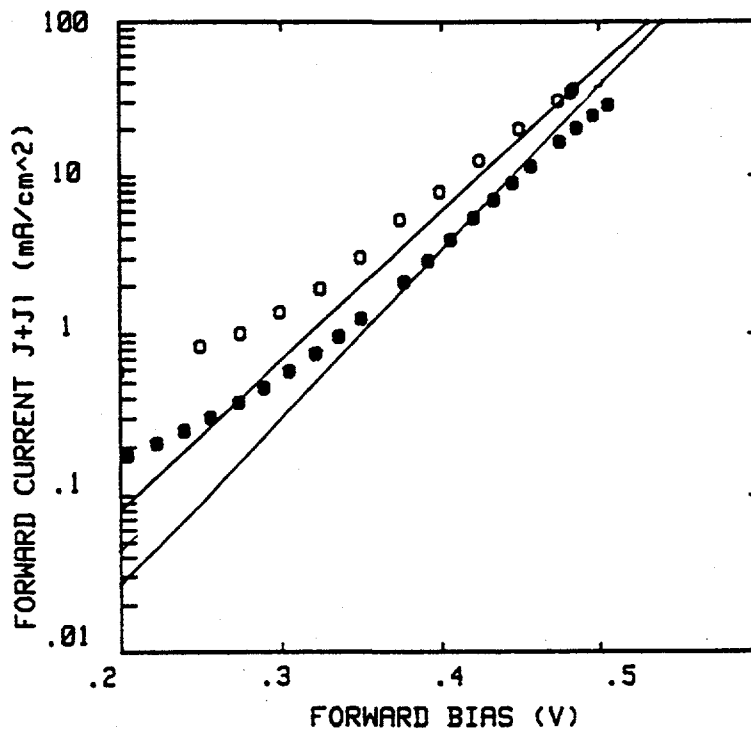


Fig. 12. Logarithmic plot of $J+J_1$ (\square) and dark I-V (\blacksquare) characteristics of the device of Fig. 10. Solid lines represent data corrected for R_s (0.2 and $0.3 \Omega\text{-cm}^2$ in light and dark, respectively).

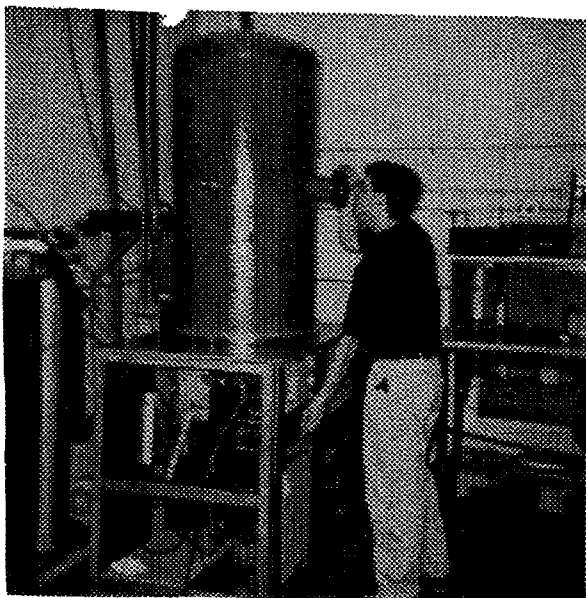
3.3. Fabrication of 1 ft² Sub-Modules

During this period we have set up in-house capability for processing 1 ft² size substrates. As a result of these efforts we have demonstrated a monolithically integrated module of 1 ft² area. The following paragraphs will briefly review the work carried out in this large area processing task.

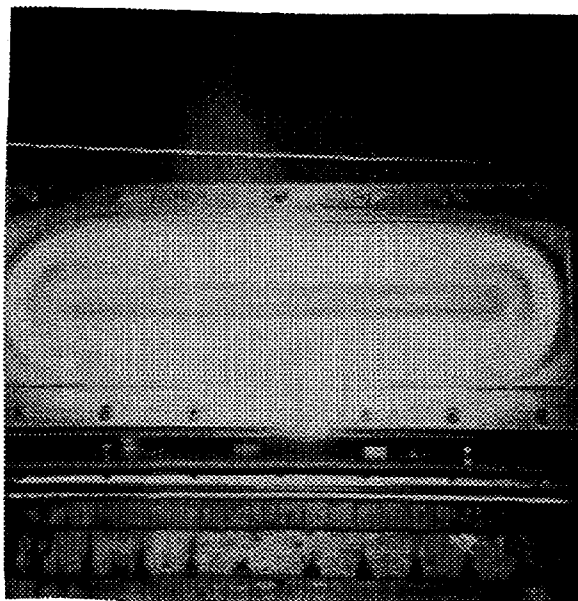
3.3.1. Precursor preparation

Most of the data presented in the previous sections were on small area films obtained by the E-Beam evaporation/selenization approach which allowed adequate thickness control for the Cu and In films deposited on small area substrates. For large area modules, however, possibility of better thickness control and improved material utilization make sputtering a more feasible approach for Cu-In precursor preparation. It is for these reasons that we have set up a sputtering system that could handle up to 1 ft² size substrates. This system has a 6" diffusion pump and two of 5"x15" size internally mounted planar magnetron cathodes. The tooling allows a single substrate to travel in front of the two cathodes which are equipped with Cu and In targets. The speed of the substrate holder can be accurately controlled and the source to substrate distance can be varied between 1 and 4 inches. A 10 kW DC power supply is employed in this system and the working gas (Ar) pressure can be controlled in the range of 1-50 mTorr during In and Cu depositions. Figure 13a shows this bell jar system. One of the planar magnetron cathodes utilized in the machine is shown in Fig. 13b. This specific cathode has a Cu target mounted on it and the race-track is visible in this photo.

Thickness uniformity and repeatability are of prime concern in the sputtering/selenization process. Uniformity of the race track along the cathode length affects the deposited film uniformity perpendicular to the axis of motion of the substrate, whereas, the surface properties of the target as well as the control over the cathode power level and the substrate speed determine the repeatability of the film thickness from run to run. There are also some basic factors which affect the film quality such as its structure and morphology. These factors are the working pressure and the sputtering power level. For Cu films, like many of the refractory metals, the pressure/structure relationships are well established (15). We also found Cu deposition by the sputtering technique to be relatively well behaved. Indium deposition, on the other hand, was more problematic. For example, under certain deposition conditions In films tended to be covered by a black powdery layer and the repeatability of their thickness from run to run was not very good. Furthermore, arcing was generally observed during the In deposition process. We have optimized some of these deposition parameters. However, there is still a need to develop a basic understanding of the In sputtering technique. Optimization



(a) The belljar system.



(b) The magnetron cathode.

Fig. 13. The sputtering system built for 1 ft² module processing.

of the In layers is especially important for our processing approach which uses an In base film to deposit the Cu layer on top. The grain structure, uniformity, density and purity of the In films have appreciable influence on the nature of the Cu-In precursor layers as we discussed in previous sections. When Cu films are deposited on black and powdery In surfaces, for example, they do not form a uniformly alloyed precursor. This may be due to the fact that excessive amount of oxygen is present in these black In surfaces. Selenizing such a non-uniform precursor results in a CuInSe₂ film with Cu-rich areas. Such areas offer shunting paths to the solar cells produced on these CuInSe₂ films.

Besides understanding the structure and chemical composition of the deposited films it is also important to optimize the thickness uniformity of the Cu and In films. The sputtering system that we established is a batch machine that we converted from an evaporator. Cathode design is of utmost importance for uniformity in such a system. Upon studies we have found a thickness uniformity of about $\pm 5\%$ for the deposited films in our system. It is clear that we have to improve this uniformity, possibly by going to a better designed cathode.

3.3.2. Selenization

A selenization reactor was designed and built to process up to six substrates of 1 ft² area in each run. Careful selection of materials for this chamber was necessary because of the reactive nature of the H₂Se gas. It was also necessary to take into account the fact that surfaces in contact with the reactive vapor needed to be kept hot to avoid premature condensation of Se on such surfaces. A gas distribution manifold with gas flow controllers and automatic valves was also built and both the flow and the temperature controllers were interfaced with a computer. A software program allowed manipulation of important process parameters such as the temperature profile (including the cooling rate) and the flow rates of various gases on the computer screen. This reactor can be totally controlled by the computer which allows repeatable results. Selenization system is located in a chemical hood and the air through this hood passes through a large volume chemical scrubber that works 24 hours a day for safety. The output of the reactor is initially cleaned by small scrubbers placed in the hood. There is also a H₂Se detector continuously sampling the air near the reactor.

3.3.3. Window layer deposition

Large area CdS and ZnO deposition systems were also developed during this period. CdS deposition system consists of a temperature controlled bath in which several 1 ft² substrates can be placed along with the commonly used meta-stable solutions of Cd and S. Uniform coatings of CdS has been obtained on large area substrates using this system without much difficulty. Material utilization in this set-up, however, needs to be improved because the process generates excessive amount of CdS powder in the meta-stable solution. Data on dip coated CdS films have been discussed in the previous sections and will not be repeated here.

The large area ZnO deposition system has been built in the form of a 14"x14" box reactor. MOCVD technique has been adapted as the deposition approach for the ZnO layers. A gas manifold monitoring and controlling the gas flows as well as their pressures over the metal-organic bubblers has been built. DEZ has been employed as the Zn source in this process. Water vapor acted as the oxygen supply. Films were deposited at a substrate temperature of 150-200 °C. Gas distribution within the reactor box is the most important factor influencing the film uniformity in our set-up. At the present time we have achieved complete coverage of 12"x12" substrates by the ZnO layer. However, the uniformity of the sheet resistance throughout the substrates requires further optimization. We can repeatably obtain ZnO coatings on large area substrates with sheet resistances in the 7-11 ohms per square range. The resistivities are in the 1-3x10⁻³ ohm-cm range for 1-3 micron thick films. Films thinner than 1 μm show specular surfaces. It is possible to obtain specular

films that are also thicker than 1 μm by adjusting the DEZ/oxidant ratio in the reactor.

3.3.4. Module integration

In our early module integration process we have used both laser scribing and mechanical scribing approaches. The following steps were carried out on 1 ft² substrates to achieve interconnection of cells (Fig. 14).

- a) A Mo layer was sputter deposited on the glass substrate. About 2 mil wide lines were scribed in this layer using a setup employing a YAG laser. Distance between the scribed lines was approximately 0.5 cm.
- b) Cu and In layers were sputter deposited over the whole substrate.
- c) The precursor was selenized at around 400 C to form CuInSe₂. A thin CdS layer was deposited over the CuInSe₂ film.
- d) Mechanical scribing was used to open grooves in the CuInSe₂ layer.
- e) ZnO was deposited to form the top contact. ZnO has also interconnected the adjacent cells through the scribes in the CuInSe₂ layer.
- f) Mechanical scribing was used to isolate the adjacent devices.

Figure 15 shows a 1 ft² module processed by the steps described above. This is one of the few 1 ft² modules we have processed in this program. These are early devices that demonstrated our ability to process a 1 ft² module from the glass substrate to the completion. The module making process itself needs further refinement and development to improve the power output. The major problems we have seen in these early modules will be discussed in the following paragraphs.

3.3.5. Further work required on module processing

The early modules we produced showed an open circuit voltage of 10-12 V and a poor fill factor. The problem areas that need further attention and development in the module processing are listed below:

- a) The uniformity of the Cu-to-In ratio along the axis of travel of the substrate does not present a problem in our sputtering system. Obtaining uniformity along this axis mainly

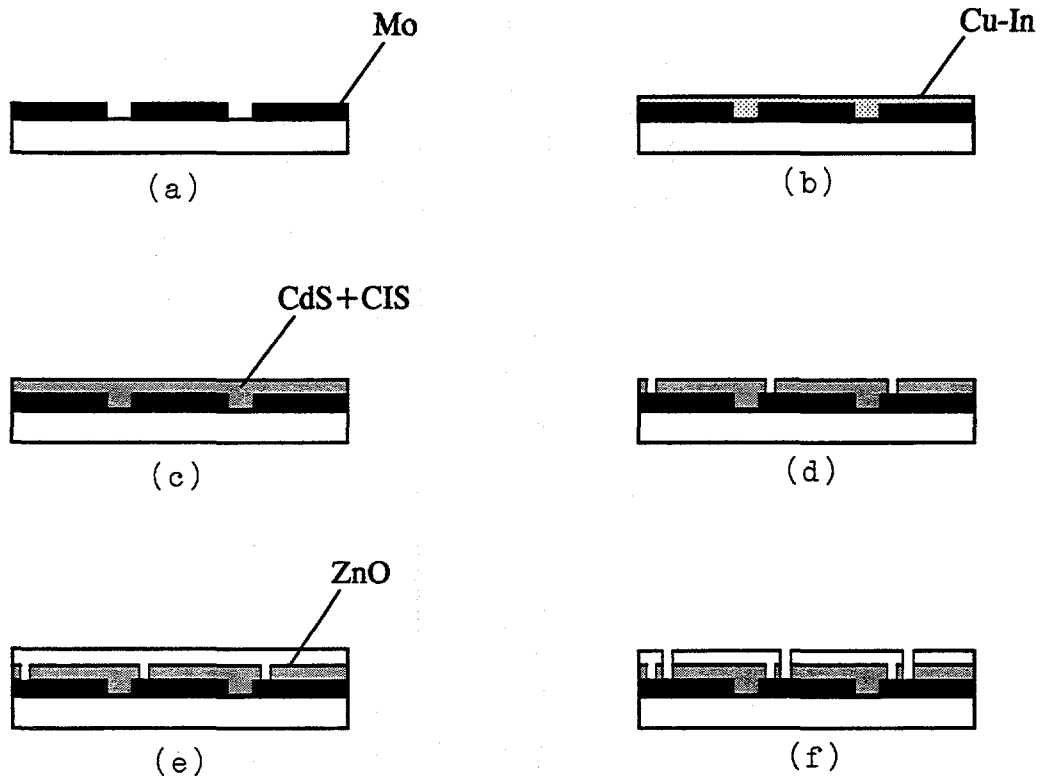


Fig. 14. Monolithic integration procedure for the modules.

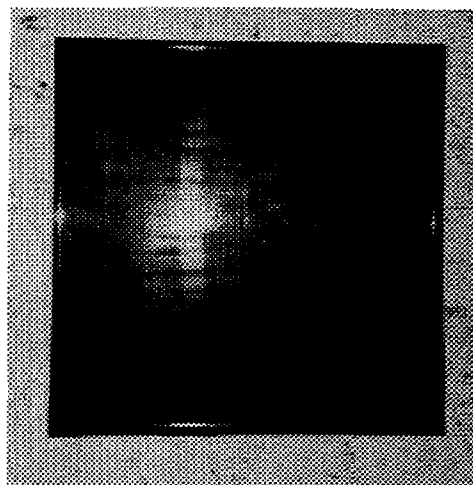


Fig. 15. Picture of a 1 ft² module processed in this program.

depends on providing a good speed control for the travelling substrate holder. Uniformity along the planar magnetron source, on the other hand, is a function of the quality of the cathode which is related to the uniformity of the magnetic field at the surface of the target. This needs to be improved in our existing system. Repeatability of Cu and In thicknesses from run to run is a function of the target surface as well as the erosion characteristics of the race-track. In our system we first sputter the target material on the shutter to condition the target surfaces before each run. The repeatability is expected to improve in a load-lock system where the targets are not exposed to the atmosphere in between runs.

b) Our approach for precursor deposition which involves deposition of a thin Te layer under the In/Cu films yields quite uniform alloy precursors. These films adhere well to their substrates and the CuInSe_2 layers obtained from such precursors also show good adhesion provided that the selenization conditions are closely controlled. However, in a module structure peeling problems are often observed especially along the scribed Mo lines. This is partially due to the imperfections left behind by the laser scribing step along the Mo scribes and partially due to the fact that adhesion between the CuInSe_2 layer and the exposed glass in the Mo grooves is not as good as the bond between the CuInSe_2 film and the Mo layer.

c) We found that the debris resulting from the laser scribing of the Mo layer very often fall into the groove and electrically short the Mo pads. Rubbing the Mo surface with a wet cotton after the laser scribing step generally cleans the grooves and removes these shorts. Laser scribing conditions need to be adjusted to reduce the formation of such debris on the scribed substrate.

d) The mechanical scribe before the ZnO deposition is an important step affecting the fill factor of the resulting devices. The Mo surface gets selenized during the formation of the CuInSe_2 film. If the mechanical scribe does not remove this selenide layer from the Mo surface, then a ZnO/Mo-selenide junction forms after the ZnO deposition. This junction is not ohmic and it reduces the fill factor of the resulting sub-module.

e) There are micro-scale non-uniformities in the photovoltaic response of cells prepared by the selenization technique. These non-uniformities can be studied using planar EBIC photographs. An example of such a study is given in Fig. 16 which compares the SEI and EBIC data of a Mo/ CuInSe_2 /CdS/ZnO device.

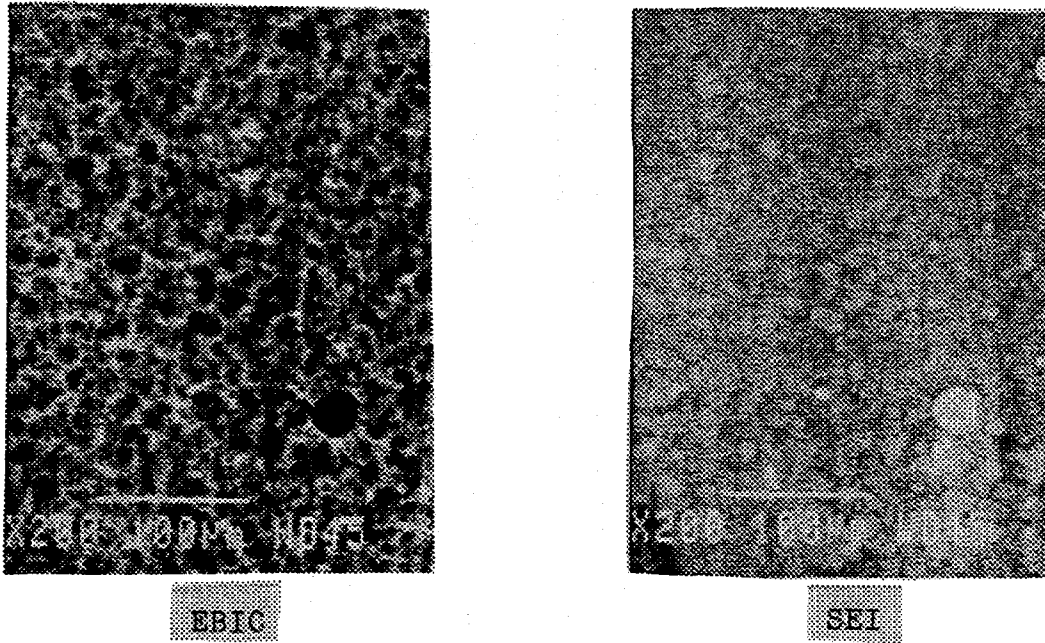


Fig. 16. EBIC and SEI data taken from a $\text{CuInSe}_2/\text{CdS}/\text{ZnO}$ device. Some of the "low-response" areas on the EBIC photo can be correlated with physical features in the SEI.

4.0 CONCLUSIONS

During this period of research we have accomplished tasks that has brought the CuInSe_2 technology closer to module manufacturing. Specifically, we have developed a novel precursor deposition approach that improved the mechanical and electrical properties of the CuInSe_2 films. As a result, we were able to raise the demonstrated device efficiency to the 12.4% range. We have established large area sputtering facility, selenization reactor, and CdS and ZnO deposition systems to handle up to 1 ft² size substrates. We have performed all the steps necessary to process a 1 ft² modules and obtained some prototypes. We have analyzed these modules and determined the steps in the module manufacturing process that need further development. Future work will concentrate on these points to improve the conversion efficiency of CuInSe_2 modules obtained by the selenization process.

5.0 ACKNOWLEDGEMENTS

The authors are grateful to R. Matson, A. Franz, A. Mason and K. Emery of NREL for SEM, Auger and I-V measurements and to Dr. H. Ullal and K. Zweibel for extensive technical discussions. Optical characterization carried out by R. Dhere and K. Ramanathan are gratefully acknowledged.

6.0 FUTURE PLANS

In this report we have discussed the processing steps for the fabrication of CuInSe_2 solar cells and modules. We have also reviewed the key issues especially in module manufacturing. Although we will continue to optimize the individual solar cell efficiencies by optimizing the window layers, future work in this program will primarily concentrate on increasing the efficiency of 1 ft^2 modules. We intend to do some modifications in our processing equipment to improve the repeatability and uniformity of Cu-In sputtering. We intend to fully develop the large area Mo sputtering capability, and improve the uniformity and resistivity of the ZnO layers deposited by the MOCVD technique.

7.0 LIST OF PUBLICATIONS

1. V.K. Kapur and B.M. Başol, "CIS solar cells by a two-stage process", International PVSEC-5, Kyoto, Japan, 1990, p. 751.
2. B.M. Başol, V.K. Kapur and R.J. Matson, "Control of CIS film quality by substrate surface modifications in a two-stage process", Proc. 22nd. IEEE PVSC, Las Vegas, Nevada, 1991, p. 1179.
3. B.M. Başol, V.K. Kapur and A. Halani, "Advances in high efficiency CIS solar cells prepared by the selenization technique", Proc. 22nd. IEEE PVSC, Las Vegas, Nevada, 1991, p. 1179.
4. V.K. Kapur and B.M. Başol, "Status of polycrystalline solar cell technologies", Proc. 22nd. IEEE PVSC, Las Vegas, Nevada, 1991, p. 1179.
5. B.M. Başol, "I-III-VI₂ compound semiconductors for solar cell applications", J. Vac. Sci. Technol., in press (1992).
6. R.G. Dhere, K. Ramanathan, T.J. Coutts, B.M. Başol and V.K. Kapur, "Optical characterization of CIS solar cells obtained by the selenization method", Proc. 22nd. IEEE PVSC, Las Vegas, Nevada, 1991, p. 1077.
7. D. Albin, J. Carapella, A. Duda, J. Tuttle, A. Tennant, R. Noufi and B.M. Başol, Proc. 22nd. IEEE PVSC, Las Vegas, Nevada, 1991, p. 907.
8. B.M. Başol, "High efficiency CIS thin film solar cells", Doga-

- Turkish J. Phys., 16, 25 (1992).
9. V.K. Kapur, "Recent developments in CIS technology", 6th. Int'l PVSEC, February 1992, p. 89.
 10. B.M. Başol, "Polycrystalline thin film compound solar cells", Doga-Turkish J. Phys., in press (1992).
 11. B.M. Başol, "CIS films and devices obtained by a two-stage process", 6th. Int'l PVSEC, February 1992, p. 1109.
 12. B.M. Başol, "CIS thin films for solar cell applications", 5th Int'l SAMPE Electronics Conf., June 1991, p. 519.
 13. V.K. Kapur, "Deposition techniques for thin film solar cells", 5th Int'l SAMPE Electronics Conf., June 1991, p. 511.

8.0 REFERENCES

1. B. M. Başol and V.K. Kapur, "High efficiency copper ternary thin film solar cells", Final Report on SERI contract No. XL-7-06031-6, March 87-July 90.
2. B. M. Başol and V. K. Kapur, Proc. 21st IEEE PVSC, 1990, IEEE, New York, p. 546.
3. B. M. Başol and V. K. Kapur, IEEE Trans. Electron. Dev., 37, 418 (1990).
4. H. Dittrich, B. Dimmler, R. Menner and H. W. Schock, Proc. 8th EC Photovoltaic Solar Energy Conf., Reidel, Dordrecht, 1988, p. 1102.
5. R. D. Varrin, S. Varma, R. W. Birkmire, B. E. McCandles and T.W.F. Russell, Proc. 21st IEEE PVSC, IEEE, New York, 1990, p. 529.
6. D. Albin, J. Carapella, A. Duda, J. Tuttle, A. Tennant, R. Noufi and B. M. Başol, Proc. 22nd IEEE PVSC, IEEE, New York, 1991, p. 907.
7. V. K. Kapur, B. M. Başol and E. S. Tseng, Solar Cells, 21, 65 (1987).
8. B. M. Başol, V. K. Kapur and R. J. Matson, Proc. 22nd IEEE PVSC, IEEE, New York, 1991, p. 1179.
9. R. F. Bunshah, "Deposition technologies for films and coatings", Noyes Publications, New Jersey, 1982.
10. A. V. Shahidi, I. Shih and H. Champness, Can. J. Phys. 63, 811 (1985).
11. M. Hansen, "Constitution of binary alloys", McGraw-Hill, 1958.
12. B. M. Başol and V. K. Kapur, U.S. Patent 5,028,274 (July 1991).
13. R. G. Dhere, K. Ramanathan, T.J. Coutts, B.M. Başol and V.K. Kapur, Proc. 22nd IEEE PVSC, IEEE, New York, 1991, p. 1077.
14. X. X. Liu, R.A. Sasala and J.R. Sites, Proc. 22nd IEEE PVSC, IEEE, New York, 1991, p. 930.
15. J. A. Thornton, J. Vac. Sci. Technol., 11, 666 (1974).

Document Control Page	1. NREL Report No. NREL/TP-413-5010	2. NTIS Accession No. DE92016438	3. Recipient's Accession No.
4. Title and Subtitle Low-Cost CuInSe ₂ Submodule Development		5. Publication Date October 1992	
		6.	
7. Author(s) B.M. Basol, V.K. Kapur, A. Halani, C. Leidholm		8. Performing Organization Rept. No.	
9. Performing Organization Name and Address International Solar Electric Technology 8635 Aviation Blvd. Inglewood, CA 90301		10. Project/Task/Work Unit No. PV231101	
		11. Contract (C) or Grant (G) No. (C) ZN-0-19019-2 (G)	
12. Sponsoring Organization Name and Address National Renewable Energy Laboratory 1617 Cole Blvd. Golden, CO 80401-3393		13. Type of Report & Period Covered Technical Report 9 July 1990 - 31 January 1992	
		14.	
15. Supplementary Notes NREL technical monitor: H.S. Ullal			
16. Abstract (Limit: 200 words) This report describes work to develop and demonstrate the processing steps necessary to fabricate high-efficiency CuInSe ₂ solar cells and submodules by the two-stage technique (also called the selenization method). We optimized the processing parameters of this method and demonstrated CuInSe ₂ /CdS/ZnO devices with 1-4 cm ² areas and up to 12.4% active-area efficiency. We also developed a novel approach for preparing Cu/In precursors that improved the stoichiometric and morphological uniformity in these films. We developed processing steps and tooling for handling up to 1-ft ² substrates and, as a result, demonstrated our first monolithically integrated submodule of 1 ft ² area.			
17. Document Analysis a. Descriptors submodules ; copper indium diselenide ; photovoltaics ; solar cells ; thin films ; modules ; low cost b. Identifiers/Open-Ended Terms c. UC Categories 273			
18. Availability Statement National Technical Information Service U.S. Department of Commerce 5285 Port Royal Road Springfield, VA 22161		19. No. of Pages 39	
		20. Price A03	